SURFACE AND INTERFACE ANALYSIS
Surf. Interface Anal. (In press)
Published online in Wiley InterScience (www.interscience.wiley.com). DOI: 10.1002/sia.2060

SIA

Interaction of O_2, CO and CO_2 with Co films

M. Frerichs, F. X. Schweiger, F. Voigts, S. Rudenkiy, W. Maus-Friedrichs and V. Kempter*

Institut für Physik und Physikalische Technologien der Technischen Universität Clausthal, Leibnizstr.4, D-38678 Clausthal-Zellerfeld, Germany

Received 4 January 2005; Revised 18 April 2005; Accepted 19 April 2005

Metastable impact electron spectroscopy (MIES), ultraviolet photoelectron spectroscopy (UPS(HeI)) and x-ray photoelectron spectroscopy (XPS) were applied to study the interaction of O_2, CO and CO_2 with Co films at room temperature. The films were produced on Si(100) surfaces under the *in situ* control of MIES, UPS and scanning tunnelling microscopy (STM). For O_2, dissociative adsorption takes place initially and then incorporation of oxygen starts at exposures of ~5 L. Comparison of the MIES and UPS spectra with those published for CoO shows that near-stoichiometric CoO films can be obtained by co-deposition of Co and O_2. The CO is adsorbed molecularly up to a maximum coverage of ~0.6 monolayer, with the C-end pointing towards the surface. The CO_2 adsorption is dissociative, resulting in the formation of Co–CO bonds at the surface. The resulting oxygen atoms are mostly incorporated into the Co layer. For all studied molecules the interaction with Co is similar to that with Ni. Copyright © 2005 John Wiley & Sons, Ltd.

KEYWORDS: MIES/UPS; XPS; STM; cobalt; adsorption

INTRODUCTION

The properties of Co films and particles and their interaction with ambient gases and vapours are of practical and fundamental interest. In the following, a few examples are mentioned:

Co is an important element in new high-temperature solid oxide fuel cells (SOFC)[1] and consequently its reaction with gas molecules from the ambient atmosphere is of practical concern.

Permanent magnets play a key role in technology and industry, ranging from the generation and distribution of electrical power to communication devices and the processing of information.[2] The magnetic anisotropy energy (MAE) is the key variable that describes the tendency of the magnetization to align along specific spatial directions. With respect to bulk solids, surface-supported nanoparticles offer additional degrees of freedom to tune the MAE by modification of the particle size, shape and coupling with the substrate. Among the 3d ferromagnetic elements hexagonal close-packed Co possesses a large MAE, particularly in the Co/Pt system, owing to the strong spin-orbit coupling of the Pt 5d states. Again, the stability of the magnetic nanoparticles against environmental gases and their influence on the MAE is of obvious interest.

The structure and stability of Co nanoparticles for ferrofluidic applications is a recent focus of interest. Here, the stability of such nanoparticles against the ambient atmosphere or fluidic environments during their production requires detailed knowledge of the Co particle–molecule interaction.[3]

The interaction of O_2 with Co single-crystal surfaces and films has been the subject of a number of studies whereby a variety of surface analytical tools were applied.[4–9] Although it is generally agreed that oxidation is preceded by dissociative oxygen chemisorption, details of the oxidation process appear to be not well understood. Cobalt oxide films on different substrates (Ag(100), Au(111) and Au(100)) were investigated with UPS, STM and scanning tunnelling spectroscopy (STS).[9–11] The structures seen in the photoelectron spectra appear to be poorly understood and so far can not be related to the density of states obtained from first-principle calculations.[12]

A few studies exist on the interaction of CO with Co surfaces[13–16] but the mechanism that leads to adsorption at room temperature is not understood; it is not even clear under which surface conditions molecular adsorption takes place. It was claimed that dissociative adsorption takes place at Co nanoparticles whereas it is non-dissociative at films.[15]

Although the interaction of CO_2 with Ni is well studied,[17,18] only little attention has been paid to the study of the interaction of CO_2 with Co.[14]

The aim of the present work is a systematic study of the interaction of Co with O_2, CO and CO_2 at room temperature by combining MIES and UPS(HeI) with XPS and STM. Owing to its inherent surface sensitivity, MIES is ideally suited for the investigation of gas–surface interactions.[19,20] With the exception of Ref. 8 no MIES data are available for the interaction of O_2, CO or CO_2 with Co. Emphasis is put on comparison of the present results with the corresponding results available for interaction with Ni.

*Correspondence to: V. Kempter, Institut für Physik und Physikalische Technologien der Technischen Universität Clausthal, Leibnizstr.4, D-3678 Clausthal-Zellerfeld, Germany.
E-mail: v.kempter@pe.tu-clausthal.de
Contract/grant sponsor: Stiftung Industrieforschung;
Contract/grant number: S 626.
Contract/grant sponsor: Deutsche Forschungsgemeinschaft;
Contract/grant numbers: SPP 1072; SPP 1153.

EXPERIMENTAL

The apparatus was described in detail previously.[21] Briefly, it is equipped with a hemispherical analyser (VSW HA 100) in combination with He*/HeI and a source for XPS providing either Al K_α or Mg K_α. Metastable impact electron spectroscopy (MIES) and UPS are performed by applying a cold-cathode discharge adapted to the ultrahigh vacuum chamber via a two-stage pumping system. A time-of-flight technique is integrated to separate electrons emitted by He* (MIES) and HeI (UPS). The MIES and UPS spectra are recorded with a resolution of 250 meV under normal emission within 100 s. The angle of incidence for the mixed He*/HeI beam is 45°. X-ray photoelectron spectroscopy is performed using a commercial x-ray source (Specs RQ20/38C). The photons hit the surface under an angle of 80° to the surface normal. Emitted electrons are analysed under 10° with respect to the surface normal, with a spectrometer resolution of 1.2 eV. The base pressure of the apparatus is 2×10^{-11} mbar.

Metastable He* atoms with thermal energy (~85% of them in the 2^3S state) can interact via three different mechanisms depending on the electronic structure of the surface and its work function (for details see Refs 19 and 20). In the present work only Auger neutralization (AN) and Auger de-excitation (AD) are observed. For metals with work functions of >3.5 eV, the first step in the interaction is the resonant transfer of the 2s electrons into unoccupied metal surface states. Subsequently, the remaining He^+ is neutralized by AN: hereby a surface electron fills the He 1s vacancy, thus emitting a second surface electron carrying the excess energy. The AN-induced MIES spectrum is a self-convolution of the surface density of states (SDOS). For metal surfaces with work functions of <3.5 eV or for wide-bandgap insulators, as with MgO for example, the interaction takes place via AD: a surface electron fills the He 1s vacancy, thus emitting the He 2s electron with excess energy; AD-type MIES spectra essentially image the SDOS. The situation is more delicate when molecular adsorption onto metals is studied. Often, a transition from AN (on clean metals) to AD takes place as a function of the adsorbate coverage because either an insulating surface is formed or transfer of the He 2s electron into the metal, which is the prerequisite for the AN process, becomes inhibited.

Co films were produced by evaporating Co bulk material with a commercial evaporator (Omicron EFM3) at a flux of ~0.65 ML min^{-1}; they were deposited on clean Si(100) targets at room temperature. The Si targets were cleaned by flashing to 1100 °C for several seconds. The absence of oxygen and other possible contaminants was verified by MIES, UPS and XPS.

The same techniques were utilized to monitor the quality of the Co films. The HeI spectra (see bottom spectra in Figs 2, 4 and 5) are very similar to Co(11$\bar{2}$0),[4] Co(0001)[5] and Co/Si(111);[15] in particular, they show no signs of emission from the Si substrate. Typical film thicknesses employed in this work are of the order of 1.4 nm, as estimated by XPS from attenuation of the Si 2s/Si 2p peaks during Co exposure. In addition, the film topology was studied by applying tunnelling microscopy. Figure 1 shows STM images of the

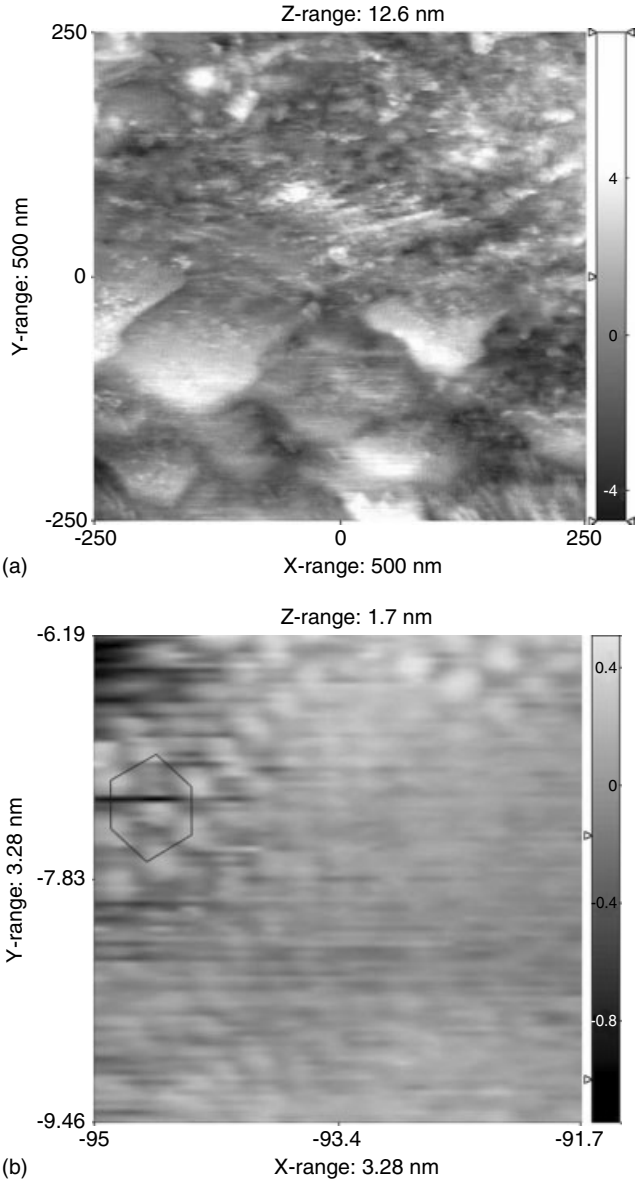

Figure 1. Scanning tunnelling microscopy images of the Co film prepared on Si(100): (a) 500 × 500 nm^2, BIAS voltage 1 V, feedback current 0.5 nA; (b) 3.28 × 3.28 nm^2, BIAS voltage 0.1 V, feedback current 1.5 nA.

Co film produced in this manner. As already concluded from the UPS data, the surface is completely covered by Co, which can be seen from a typical image with of size 500 × 500 nm^2 (Fig. 1(a)). Part of the layer consists of Co particles (see top area). Other regions are covered by a flat Co layer displaying the geometry of Co(0001) (see Fig. 1(b) for identification of the Co(0001) unit cell).

Cobalt oxide films were produced by Co evaporation at a rate of ~0.1 ML min^{-1} in an oxygen partial pressure of 5×10^{-7} mbar at a sample temperature of 370 K; the conditions are similar to those employed for the production of CoO films on Au(111).[10] Subsequently, the sample was heated at 5×10^{-7} mbar at 370 K for 5 min without further Co supply. Even at oxygen saturation the contributions from metallic Co are still visible in the UPS spectra. Taking the finite depth resolution of UPS into account we estimate that

the CoO layer possesses a thickness of <3 ML. Also on Ni(100) surfaces the formation of oxide layers appears to be limited to a thickness of ~3 ML at room temperature.[22]

Neither the Si(100) sample nor the ultrathin adlayers cause any charge-up problem, therefore, the surface work function and the work function changes (ΔWF) could be determined from the low-energy onset of the MIES or the HeI spectra with an accuracy of ±0.1 eV. All spectra are displayed as a function of the electron binding energy with respect to the Fermi level, E_F, which is determined by the high-energy cut-off obtained on metallic samples in UPS and MIES.

RESULTS

Oxygen interaction with Co films

Figure 2 shows the MIES and UPS(HeI) spectra collected during the interaction of O_2 at room temperature with a Co film produced in the manner described above. The bottom spectra are for clean Co. The UPS(HeI) spectra are dominated by a strong emission at and below E_F that is due to ionization of Co 3d states of metallic Co. The MIES spectra in contrast are less structured because the interaction between He^* and the Co surface is apparently dominated by AN, as shown by comparison with the MIES spectra from Ni(100).[19,23] Both the MIES and UPS results are very similar to the corresponding results obtained from Ni(100) surfaces.[22] With increasing oxygen exposure both UPS and MIES display structures that are related to the beginning of oxidation of the Co film. In Fig. 2 we have indicated the energy positions of features A–E: A, 1.9 eV; B, 3.7 eV; C, 5.0 eV; D, 6.8 eV; E, 11.3 eV. Similar structures are seen at these positions in the UPS spectra for Co interacting with O_2[9–11] (our notation follows this work) for $LaCoO_3$[24] and for NiO.[19,22] The surface appears to be saturated at an exposure of ~500 L. Even for $>10^3$L UPS still displays intensity at E_F. The origin of the shoulder (seen between E_F and $E_B = 1$ eV) will be discussed below.

In order to relate the structure developing during the O_2 exposure, we compare the MIES and UPS spectra for O_2/Co with those from a CoO film produced on Si(100) as described in the Experimental (Fig. 3). The positions A–E introduced in connection with Fig. 2 are also displayed. Our UPS spectra for CoO agree well with those for CoO(100),[8] CoO films on Au(111)[9] and CoO films on Au(001).[11] The energy positions of the UPS structures seen for CoO agree well with those seen for NiO, and are very close to A–E. Structures occur also in the MIES spectra at similar energies but only a weak shoulder appears in the region of A and B. The structure found in the region of C and D is considerably narrower in MIES. On the other hand, feature E, which is weak in UPS, appears rather pronounced in MIES. Similar behaviour was found for $LaCoO_3$[24] and NiO surfaces.[23] If AN were to take place at the CoO surface, pronounced structures in the MIES spectrum, such as seen in Fig. 3, would not be expected. This forbids attributing the differences seen between MIES and UPS to the occurrence of the AN process. As was done for $LaCoO_3$,[24] we attribute the MIES spectrum for CoO to the AD process. Later an attempt will be made to relate the MIES and UPS spectra and to come to an interpretation of features A–E.

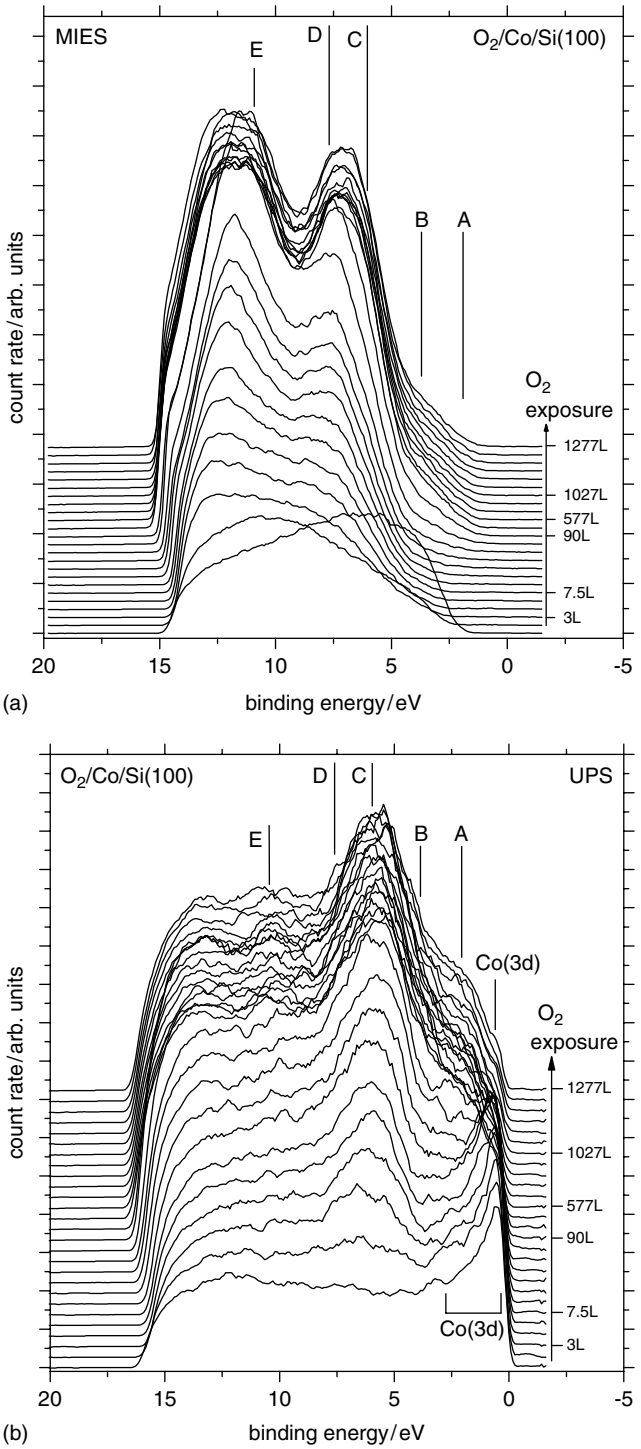

Figure 2. The MIES (a) and UPS (b) spectra during interaction of O_2 with Co films. The meaning of A–E and Co 3d is explained in the text. Oxygen was introduced at a constant rate between any of two adjacent exposure values; accordingly, the exposure rate increases from the bottom to the top.

Weak emission is seen in the UPS spectrum in Fig. 3 between E_F and $E_B = 1$ eV; in Fig. 2(b) a comparatively strong shoulder shows up in the same region. Angle-resolved UPS spectra on 10 ML CoO, grown on Au(111) in an oxygen atmosphere,[10] do not show this emission. Moreover, soft XPS was applied to thin Ni films deposited on $SrTiO_3$(100), interacting with oxygen.[25] Before the complete

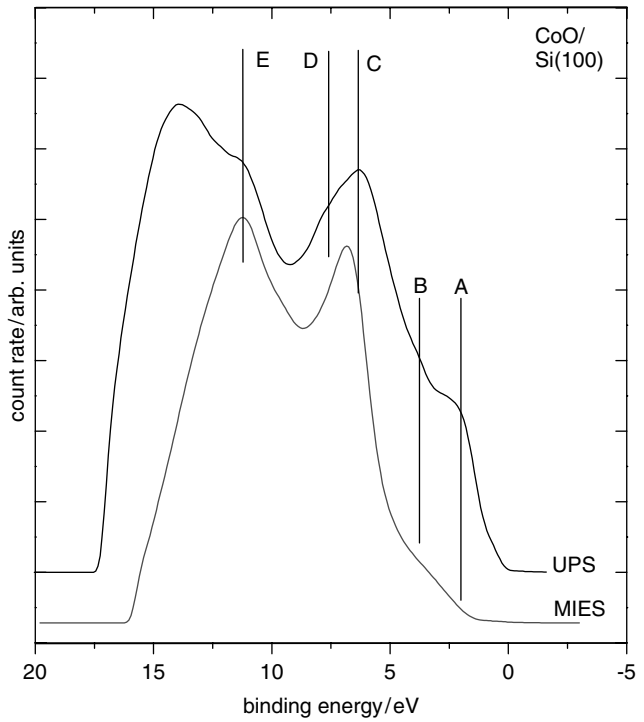

Figure 3. The MIES and UPS spectra of a CoO film produced by Co–O_2 co-deposition. The meaning of A–E and Co 3d is explained in the text.

transformation of the originally metallic Ni overlayer into NiO as a function of oxygen exposure at room temperature has taken place, emission is seen between E_F and $E_B = 1$ eV, which is attributed to emission from Ni 3d states.[25] For the thin Ni films employed in Ref. 25 the Ni 3d-induced emission reappears after annealing the NiO film to 850 K. The results of Refs 10 and 25 suggest that the weak emission seen in Fig. 3 between E_F and $E_B = 1$ eV and the shoulder seen in the same region in Fig. 2(b) are caused by contributions from metallic-like Co 3d states originating from subsurface Co atoms.

Interaction of CO with Co films

Figure 4 shows MIES and UPS spectra for the interaction of CO with a Co film produced as described earlier. The bottom spectra are for clean Co. Already at an exposure of 2 L strong changes occur in the MIES spectra. Two structures develop at $E_B = 7.8$ and 11.1 eV. These peaks are, as in the case of Ni, attributed to ionization of the CO $1\pi/5\sigma$ and 4σ molecular orbitals.[26] Although the peak positions are very similar in MIES and UPS, their intensity ratio is quite different. The fact that the MIES spectra developing during CO exposure display sharp structures at about the same binding energies as UPS strongly suggests that they are due to AD. Apparently, CO molecules located on top of the surface modify the interaction between the He^* 2s orbital and the surface, thus inhibiting the resonant transfer of the 2s electron into unoccupied states of the surface, which would be the initial step of the AN process. From the decrease of the metallic Co 3d emission (emission seen near E_F) we can estimate the CO saturation coverage to ~3 L. Our estimate is based on the following facts: in UPS(HeI) the Co 3d metallic

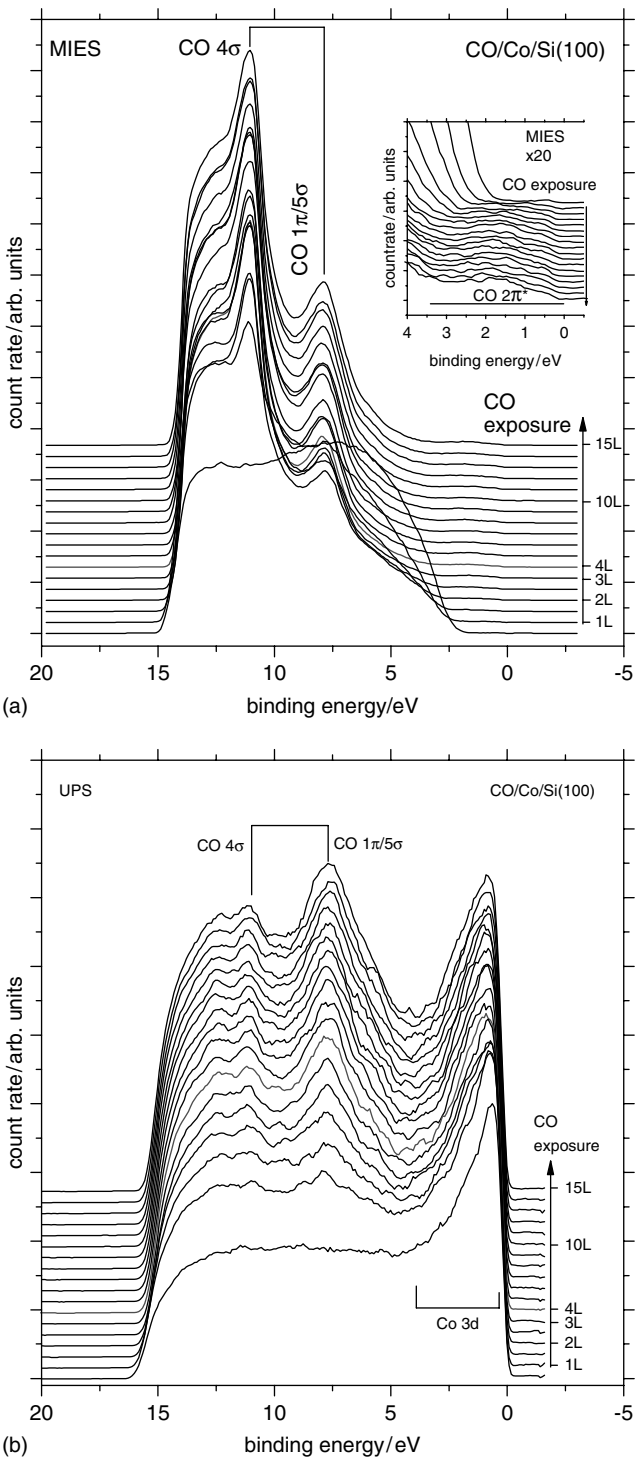

Figure 4. The MIES (top) and UPS (bottom) spectra during interaction of CO with Co films. Inset shows details for binding energies up to 4 eV. Carbon monoxide was introduced at a constant rate between any of two adjacent exposure values; accordingly, the exposure rate increases from the bottom to the top.

contribution is barely attenuated, therefore the CO coverage is <1 ML; and with MIES we see no emission that could be attributed to ionization of Co 3d in the metallic environment, therefore, those Co species must be shielded against access by the He^* probe atoms. Combining these two facts allows us to conclude that at room temperature CO saturation occurs

below but close to a monolayer. Additional information on the coverage comes from XPS.

The inset in Fig. 4(a) shows a magnification of the MIES spectra for 4 eV < E_B < E_F; the top spectrum corresponds to zero exposure and the bottom spectrum to 15 L. A similar spectral feature developing during the adsorption of CO on Pd, Cu, Ni and Ru has been reported previously[20] and was attributed to the population of the CO $2\pi^*$ antibonding molecular orbital.

Interaction of CO_2 with Co films

Figure 5 presents the MIES and UPS spectra obtained during interaction of the Co film with CO_2, starting with the clean Co film (bottom spectra). Peaks appear in MIES and UPS, which, as comparison with Fig. 4 shows, have to be attributed to emission from the CO $1\pi/5\sigma$ and CO 4σ molecular orbitals. Carbon dioxide chemisorption via CO_3^{2-} formation would result in three structures at E_B = 6.9 11.5 and 13.3 eV.[27] Activation of CO_2 via CO_2^- formation would lead to the appearance of three structures at positions similar to those for CO_3^{2-}.[28] We conclude that, as for the interaction of CO_2 with Ni (100).[18] CO_2 dissociation takes place during the interaction, resulting in the formation of Co–CO bonds. At room temperature saturation is reached at ~200 L, the coverage then being comparable to that for CO.

Work function and XPS studies

The work function of the clean Co film amounts to 5.0 ± 0.1 eV and corresponds well to the photoelectrically measured work function of 5.0 eV for Co bulk material.[29,30] It can be compared with the value of 4.7 eV for a Co film of 5 ML thickness on Pt(111).[31] We attribute the difference of 0.3 eV to the different surface structure and roughness.

Figure 6 shows the work function change (ΔWF) versus exposure for the interaction with the studied gases. The error bars result from the uncertainty in the determination of the cut-offs in the spectra. Similar to what was found for oxygen adsorption on Co(11$\bar{2}$0), the work function increases initially by 0.43 eV, followed by a decrease to a saturation value 0.37 eV below the work function of the Co film. This behaviour was attributed to dominant chemisorption in the initial phase of oxygen interaction, followed by oxygen incorporation into the Co lattice.[6] In saturation, the work function is still ~1 eV larger than expected for bulk-like CoO films.[4,10] During CO exposure the initial work function increase is 0.55 eV, saturating at 3 L. For CO_2 the work function increases by 0.87 eV and saturates at 30 L.

From XPS measurements (not shown here) we have estimated the intensity ratios of the O 1s and the Co L_3VV peaks in the cases shown in Figs 2–5 (from the bottom to the top). Additional information on the stoichiometry of the Co films exposed to gases could be obtained from analysis of the Co 2p peaks.[32] We have also applied XPS to a Co film exposed to 15 L CO and post-oxygenated with 200 L (see Table 1). The peak ratios for the completely oxygen-saturated Co film and the film exposed to both CO and O_2 are comparable. Both do not show the value for the stoichiometric CoO film, displaying an O 1s/Co L_3VV peak ratio of 0.32 (see Table 1). The oxygen-saturated Co film (corresponding to Fig. 1) as well as the CO-saturated (corresponding to Fig. 4) and subsequently oxidized Co films show peak ratios of ~0.24. Consequently, these Co films are not completely saturated with oxygen during oxygen exposure. In the present work a completely saturated film is only obtained during simultaneous Co and oxygen exposure at 370 K.

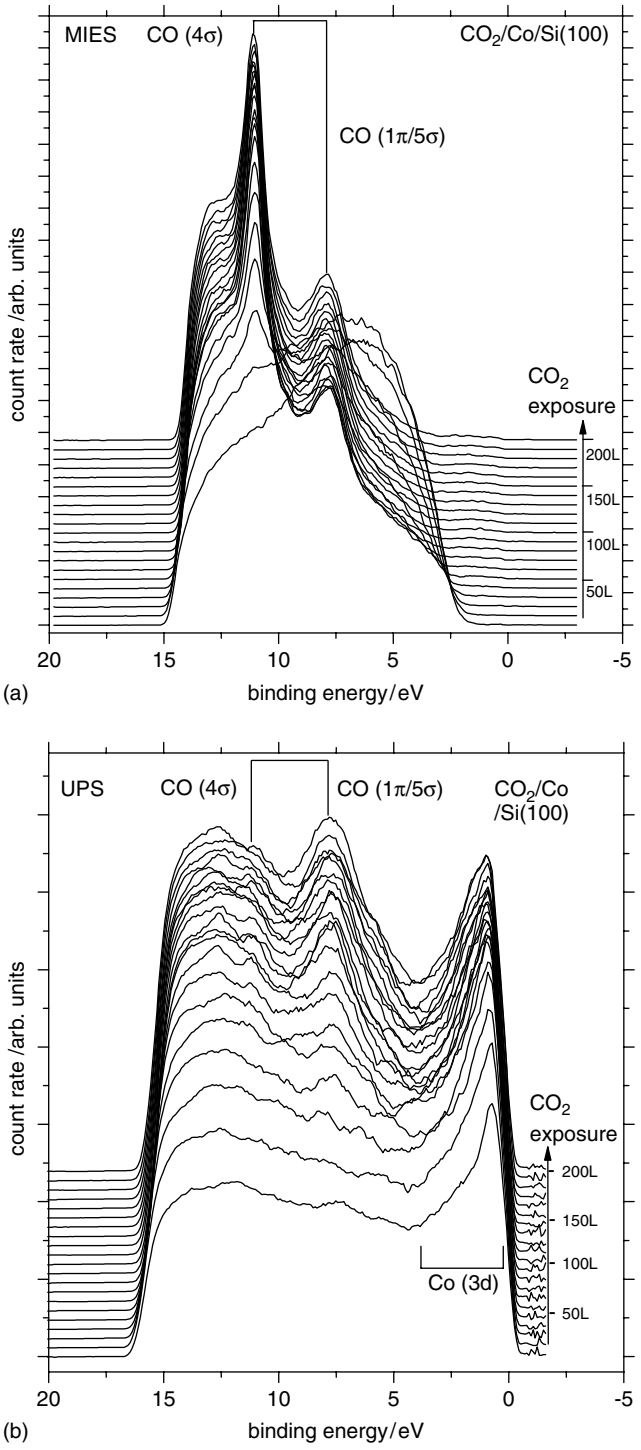

Figure 5. The MIES (top) and UPS (bottom) spectra during interaction of CO_2 with Co films. Carbon dioxide was introduced at a constant rate between any of two adjacent exposure values; accordingly, the exposure rate increases from the bottom to the top.

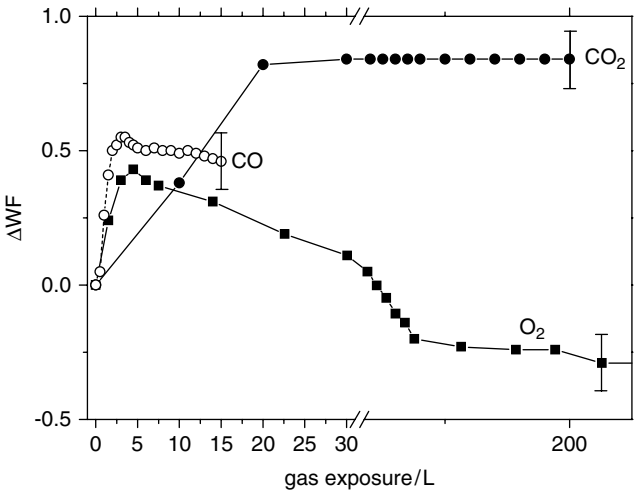

Figure 6. Work function change, (ΔWF) during the interaction of O_2, CO and CO_2 with Co films. The work function of the clean Co film is 5 eV.

Table 1. Peak ratios of O 1s/Co L_3VV for different gas exposures to a Co film

Adsorption system	Peak ratio O 1s/Co LMM_1
1300 L O_2/Co	0.26 ± 0.12
15 L CO/Co	0.08 ± 0.04
200 L CO_2/Co	0.15 ± 0.07
15 L CO/Co + 200 L O_2	0.23 ± 0.12
CoO	0.32 ± 0.16

Carbon monoxide saturation gives an O 1s/Co L_3VV ratio of 0.08. On the basis of our XPS data presented for CO in Table 1 we can give a rough estimation: a nearly stoichiometric CoO gives an O 1s/Co LMM ratio of 0.32 ± 0.16. Its thickness has been estimated to be <3 ML (see above). Following this, a Co surface completely covered with 1 ML of CO should give an O 1s/Co LMM ratio of $0.32/3 \sim 0.11$. The measured value of 0.08 ± 0.04 therefore suggests a CO coverage of ~0.75 monolayers. This supports the estimate arrived at from analysis of the MIES/UPS data.

DISCUSSION

Interaction of Co with O_2

During the initial stage of oxygen exposure MIES shows a strong and immediate decrease of the intensity attributed to the AN process involving the Co 3d states of metallic Co. Instead, a new structure appears both in MIES and UPS close to the positions of A–E. Above ~20 L, the gradual growth of spectral structures characteristic for CoO formation can be noticed both in MIES and UPS. We suggest that with increasing oxygen exposure the interaction process in MIES switches from AN to AD, involving Co and O species in a non-metallic environment. Around 3 L the work function passes its maximum, suggesting that oxygen incorporation starts at these exposures (see previous section). Summarizing, our observations are consistent with the assumption that initially oxygen species become chemisorbed before the oxidation process starts.[5]

At 300 L both the MIES and UPS spectra already display all the spectral structures seen for CoO films (Fig. 3). According to MIES (cf. Figures 2 and 3), the electronic structure of the top layer is already rather similar to that of CoO. However, in contrast to MIES, UPS still shows considerable emission in the region between E_F and A (see Fig. 2(b)). We attribute the shoulder seen in UPS between E_F and A to metallic-like 3d-states of Co species located underneath the surface (see discussion of Fig. 3 in Results section). Support for the formation of only an ultrathin CoO film comes from the fact that the work function at saturation (4.7 eV) is still considerably larger than for CoO (3.7 eV). The formation of only a thin oxide-like film reduces the probability for electron tunnelling from the metallic layer through the surface oxide; consequently, the probability for O_2 dissociation and further progress of the oxidation process become inhibited.

In the following, we discuss the structures located near the positions A–E seen in UPS and MIES for CoO as well as for O_2 adsorption on the Co film. Our results can be compared with MIES and UPS studies on thin films of NiO grown on Ni(100).[19] and those reported by the same group for NiO(100);[22] in both cases structures A–E were seen. As in the case of Ni, the emission, between 1 and 4 eV attributed to ionization of 3d states[22,23] (structures A and B) is rather weak in MIES compared with UPS. It was pointed out that the Ni^{2+} 3d orbital is rather localized whereas the O 2p orbitals are rather diffuse, as also evidenced by the large dispersion of the corresponding valence band,[33] and therefore protrude outside the surface. The activity of an orbital in MIES reflects its electron density at the position of the He probe atom at distances of the order of 2 Å in front of the layer that terminates the surface.[19,20] Therefore, it was anticipated that He^+ interaction takes place with the O 2p rather than with the more localized Ni^{2+}3d orbitals.[19,22] We assume a similar behaviour for CoO and will discuss this point later in detail.

The MIES and UPS(HeI) spectra were reported for polycrystalline $LaCoO_3$.[20,24] Both spectra display a close similarity to those for CoO (Fig. 3) and NiO[22] (featuring five structures denoted by (1)–(5) in Refs 20 and 24). The main characteristics of the spectra can be summarized as follows: as in the present results, the Co 3d-derived bands (A and B in our notation) are strongly suppressed in MIES relative to the O 2p-derived structures C and D. Also, as in the present MIES results, peak E appears considerably enhanced compared to that in UPS.

For O_2/Ni(100), NiO and $LaCoO_3$ the MIES spectra were attributed to the AD process.

To arrive at a consistent interpretation of both the MIES and UPS spectra for CoO on the basis that the MIES spectra are due to the AD process, we adapt the interpretation given in Ref. 24 to our situation. Hereby, we suppose that the Co^{2+} ions in CoO are in a local environment similar to that felt by the Co^{3+} ions in $LaCoO_3$.[20,24] The Co^{2+} 3d atomic orbitals are rather compact (1.58 atomic units) compared with the diffuse O 2p orbitals in O^{2-} (2.8 atomic units). Consequently, He^* can be expected to interact efficiently with the outermost O 2p orbitals, protruding farthest into the vacuum, rather than with the Co^{2+} 3d orbitals; (p → d) transitions (from

ionization of O 2p) will appear comparatively pronounced compared with (d → d) transitions (involving Co^{2+}3d). In the following, we consider a Co_2O_{11} cluster as model for CoO, as was done for $LaCoO_3$ in Ref. 24. The cluster includes two Co ions that are embedded into an octahedral oxygen environment, $O_5Co_AOCo_BO_5$ (see Ref. 20 for a more detailed discussion): (d^7d^7) denotes the ground-state configuration of the two Co ions in the Co_2O_{11} cluster; (d^6Ld^8) is a configuration where the transfer of a O 2p electron to one of the Co ions has taken place; L denotes a vacancy located at an oxygen species close to the Co^{2+} ions;[20,24] and (d^6d^8) represents a configuration in which the transfer of a Co 3d electron has taken place between the two Co ions of the Co_2O_{11} model cluster. The initial state is a superposition of these three configurations.[20] We propose the following assignment of the observed structures: A and B correspond to the (d → d) transitions ($d^7d^7 \rightarrow d^6d^7$) and are therefore seen only weakly in MIES; C, D, and E are due to the (p → d) transitions ($d^7d^7 \rightarrow d^7Ld^7$) and ($d^6d^8 \rightarrow d^6Ld^8$), respectively, and for this reason are seen strongly in MIES. The peak assignment proposed above is at variance with that of Ref. 10, solely based on UPS work: angle-resolved UPS spectra were collected from CoO films (thickness 10 ML, grown on Au(111) at 350 K). It was proposed[10] that A and B are due to a (d → p) transition leading to a (d^7 Ld^7) final-state configuration, and that their separation is due to crystal or ligand field splitting. As proposed above, states C and D were assigned to emission from states of the O 2p bands, i.e. to (p → d) transitions. Again, in contrast to the present interpretation, peak E was attributed to unscreened emission from Co 3d states, i.e. to a (d → d) transition. This assignment does not offer a straightforward way to explain the rather different intensities in MIES and UPS.

Interaction of Co with CO and CO_2

For most of the metals, molecular adsorption of CO occurs via its 5σ molecular orbitals whereby the C-end of the molecule points towards the surface.[10] Our MIES results show a strong enhancement of CO 4σ relative to CO 1π compared with UPS. The same behaviour was seen for CO/Ni(110) at 120 K.[20,23,26] In that case the intensity of the 4σ-derived band increased up to 0.66 ML but decreased remarkably at larger coverages. In order to explain the enhancement of the 4σ-derived band seen in MIES, we follow the suggestion made in Refs 20,22 and 26 that the CO 4σ molecular orbital stands up normal to the surface, thus protruding the most into the vacuum. This enhances its interaction probability with the impinging He^* atom. Consequently, its intensity relative to that of 1π/5σ is enhanced compared with UPS. Our MIES spectra for CO/Co at room temperature in saturation (reached at ~3 L; see also the work function results in Fig. 6) correspond to those obtained at 0.66 ML for CO/Ni at 120 K. This is consistent with our estimate for the CO coverage at room temperature of <0.75 ML made earlier.

From MIES we concluded that the CO 2π^* antibonding molecular orbital is populated (Fig. 4(a)). For CO/Ni, several models were discussed that can account for the population of the CO 2π^* antibonding molecular orbital as a consequence of the CO interaction with metals.[20] Among these, one model assumes the back-donation of surface d-electrons into 2π^*, as proposed originally in Ref. 34. For CO/Co, support of this model comes from the observed increase of the surface work function upon CO adsorption, signalling a transfer of charge from the surface to the adsorbate. Thus, the work function becomes constant when additional CO cannot be adsorbed anymore (above ~3 L). Other models take into account the hybridization of 2π^* with the broad Co valence band or the interaction between the CO adsorbate and the impinging He^* atom.[20]

As for CO_2 on Ni,[18] dissociation of impinging CO_2 into CO and O is observed on Co surfaces; the CO molecules resulting from dissociation of the impinging CO_2 molecules are adsorbed on top of the Co surface. The observed increase of the work function is at least partly ascribable to the charge transfer from the Co film to the dissociation product CO. For CO_2, saturation is achieved at ~200 L instead of at 2 L for CO. The different behaviour may be due to a low sticking probability and/or a low probability for dissociation of CO_2 at room temperature. The XPS ratios for CO saturation and CO_2 saturation (see Table 1) indicate that almost all of the oxygen atoms arising from the dissociation are incorporated into the Co film.

A two-step mechanism was proposed to explain the CO_2 dissociation on Sr:[27] the incorporation of oxygen atoms in the metallic layer, suggested by the occurrence of a peak at $E_B = 5.0$ eV; and the formation of carbonate (CO_3^{2-}) on top of the surface. In contrast, we observe no indications for this two-step mechanism in the present case: no peak at $E_B = 5.0$ eV in MIES and no peak structure characteristic for CO_3^{2-}. The information available for CO_2/Ni(110) provides a hint concerning the mechanism that may underly the observed CO_2 dissociation:[18] in this case, physisorption is limited to temperatures below 200 K. The work function increase observed during CO_2 exposure was attributed to the formation of CO_2^- species on the basis of vibrational spectroscopy; these chemisorbed species was found stable up to 150 K. At higher temperatures they became highly reactive: the CO_2^- intermediates appear to dissociate into chemisorbed CO and O atoms, as evidenced from the presence of strong CO losses and O surface vibrations at 270 K. The observed rise of the work function versus CO_2 exposure, seen also in the case of Co, may be evidence that the mechanism for CO_2 dissociation on Co films involves a CO_2^- intermediate that, at room temperature, decays into CO and O. In principle, MIES measurements carried out below 150 K could provide additional information on the eventual formation of a CO_2^- intermediate if it is long-lived enough to be accessible to electron spectroscopies.

SUMMARY

Co films were deposited on Si(100) substrates at room temperature under the *in situ* control of MIES, UPS and STM. The interaction of the films with O_2, CO and CO_2 was studied with MIES, UPS with HeI, XPS and work function measurements.

For O_2, the interaction takes place in two steps: initially, impinging O_2 is, after dissociation, chemisorbed at the

surface. Exposures larger than about 5 L lead to oxygen incorporation into the Co layer and to the onset of Co oxidation. Near-stoichiometric CoO films were produced by Co deposition in an oxygen atmosphere at 370 K. The spectra, both for Co–O_2 interaction and for Co–O_2 co-deposition, are rather similar to those with Ni instead of Co. Characteristic differences seen in MIES and UPS from CoO are attributed to the different sensitivity of the two techniques for detection of the Co 3d and O 2p states of surface-near species. The simultaneous use of MIES and UPS(HeI) allows for a more reliable identification of the spectral features seen in the valence-band spectra from CoO.

Carbon monoxide is adsorbed molecularly up to saturation at ~1 ML; no dissociation is observed. Comparison of the MIES and UPS spectra gives detailed information on the adsorption geometry: from the strong enhancement of the 4σ emission in MIES (compared with UPS) it is concluded that the CO species adsorb with the C-end pointing towards the surface, allowing the CO 4σ molecular orbital to protrude farthest into the vacuum; this enhances its interaction probability with the impinging He^* atom. The combination of work function and MIES results suggests that back-donation of charge from the Co film into the CO $2\pi^*$ antibonding molecular orbitals plays an important role in the adsorption process.

Carbon dioxide dissociates into CO and O as a consequence of interaction with the Co surface. The CO_2 dissociation leads to adsorption of CO at the surface and the incorporation of O atoms into the Co film.

For all three studied molecules the interaction with Co films is similar to their interaction with Ni.

Acknowledgements

V.K. and W.M.F. gratefully acknowledge illuminating discussions with Drs S.D. Foulias, M. Kamaratos and D. Vlachos (University of Ioannina) on the occasion of their visits at Clausthal University of Technology within the IKYDA program. Financial support by the Stiftung Industrieforschung under contract S 626 (W.M.F.) and by the Deutsche Forschungsgemeinschaft within SPP 1072 (V.K.) and SPP 1153 (S.R.) is gratefully acknowledged.

REFERENCES

1. van Hassel BA, Kawada T, Sakai N, Yokokawa H, Dokiya M, Bouwmeester HJM. *Solid State Ionics* 1993; **66**: 295.
2. Gambardella P, Rusponi S, Veronese M, *et al*. *Science* 2003; **300**: 1130.
3. Rudenkiy S, Frerichs M, Voigts F, Maus-Friedrichs W, Kempter V, Brinkmann R, Matoussevitch N, Brijoux W, Bönnemann H, Palina N, Modrow H. *Appl. Organomet. Chem.* 2004; **18**: 553.
4. Klingenberg B, Grellner F, Borgmann D, Wedler G. *Surf. Sci.* 1993; **296**: 374.
5. Castro GR, Küppers J. *Surf. Sci.* 1982; **123**: 456.
6. Grellner F, Klingenberg B, Borgmann D, Wedler G. *J. Electron Spectrosc. Relat. Phenom.* 1995; **71**: 107.
7. Gazzadi GC, Borghi A, di Bona A, Valeri S. *Surf. Sci.* 1998; **402–404**: 632.
8. Förster S, Baum G, Müller M, Steidl H. *Phys. Rev. B* 2002; **66**: 134 427.
9. Heiler M, Chassé Y, Schindler K-M, Hollering M, Neddermeyer H. *Surf. Sci.* 2000; **454–456**: 36.
10. Sindhu S, Heiler M, Schindler K-M, Neddermeyer H. *Surf. Sci.* 2003; **541**: 197.
11. Hagendorf Ch, Shantyr R, Meinel K, Schindler K-M, Neddermeyer H. *Surf. Sci.* 2003; **532–535**: 346.
12. Anisimov VI, Aryasetiawan F, Lichtenstein AI. *J. Phys.: Condens. Matter* 1996; **9**: 767.
13. Getzlaff M, Bansmann J, Schönhense G. *J. Chem. Phys.* 1995; **103**: 6691.
14. Jugnet Y, Hollinger G, Pertosa P, Porte L, Tuc TM. *J. Microsc. Spectrosc. Electron.* 1976; **1**: 187.
15. Bogdányi G, Zsoldos Z, Petó G, Guczi L. *Surf. Sci. Lett.* 1994; **306**: L563.
16. Lathinen J, Kauraala JVK. *Surf. Sci.* 1998; **418**: 502.
17. Solymosi F. *J. Mol. Catal.* 1991; **65**: 337.
18. Freund H-J, Roberts MW. *Surf. Sci. Rep.* 1996; **25**: 225.
19. Morgner H. *Adv. At. Mol. Opt. Phys.* 2000; **42**: 387.
20. Harada Y, Masuda S, Ozaki H. *Chem. Rev.* 1997; **97**: 1897.
21. Brause M, Braun B, Ochs D, Maus-Friedrichs W, Kempter V. *Surf. Sci.* 1998; **398**: 184.
22. Kubiak R, Morgner H, Rakhovskaya O. *Surf. Sci.* 1994; **321**: 229.
23. Lee J, Arias J, Hanrahan CP, Martin RM, Metiu H. *Phys. Rev. Lett.* 1983; **51**: 1991.
24. Masuda S, Aoki M, Harada Y, Hirohashi M, Watanabe Y, Sakisaka Y, Kato H. *Phys. Rev. Lett.* 1993; **71**: 4212.
25. Kamaratos M, Vlachos D, Foulias SD, Argirusis Ch. *Surf. Rev. Lett.* 2004; **11**: 419.
26. Lee J, Hanrahan CP, Arias J, Martin RM, Metiu H. *Phys. Rev. Lett.* 1983; **51**: 1803.
27. Maus-Friedrichs W, Gunhold A, Frerichs M, Kempter V. *Surf. Sci.* 2001; **488**: 239.
28. Vines F, Borodin A, Höfft O, Kempter V, Illas F. *J. Phys. Chem.* 2005; (under review).
29. http://hyperphysics.phy-astr.gsu.edu/hbase/tables/photoelec.html.
30. http://environmentalchemistry.com/yogi/periodic/Co.html.
31. Alnot M, Fusy J. *Appl. Surf. Sci.* 1992; **55**: 209.
32. Jiménez VM, Espinós JP, González-Elipe AR. *Surf. Interface Anal.* 1998; **26**: 62.
33. Kuhlenbeck H, Odörfer R, Jaeger R, *et al*. *Phys. Rev.* 1991; **B43**: 1969.
34. Blyholder G. *J. Phys. Chem.* 1946; **10**: 2772.